Variations on calculating left-ventricular volume with the radionuclide count-based method

Kenneth F. Koral,[a] Mark A. Rabinovitch, Victor Kalff, William Chan, Jack E. Juni, Bruce Lerman, Richard Lampman, Joseph Walton, Robert Vogel, Bertram Pitt, and James H. Thrall
Division of Nuclear Medicine, University of Michigan Medical Center, Ann Arbor, Michigan 48109

(Received 30 May 1984; accepted for publication 30 August 1984)

Various methods for the calculation of left-ventricular volume by the count-based method utilizing red-blood-cell labeling with ^{99m}Tc and a parallel-hole collimator are evaluated. Attenuation correction, linked to an additional left posterior oblique view, is utilized for all 26 patients. We examine (1) two methods of calculating depth, (2) the use of a pair of attenuation coefficients, (3) the optimization of attenuation coefficients, and (4) the employment of an automated program for expansion of the region of interest. The standard error of the estimate (SEE) from the correlation of the radionuclide volumes with the contrast-angiography volumes, and the root-mean-square difference between the two volume sets at the minimum SEE are computed. It is found that optimizing a single linear attenuation coefficient assumed for attenuation correction best reduces the value of the SEE. The average of the optimum value from the end-diastolic data and that from the end-systolic data is 0.11 cm^{-1}. This value agrees with the mean minus one standard deviation value determined independently from computed tomography scans ($0.13 - 0.02$ cm^{-1}). It is also found that expansion of the region of interest beyond the second-derivative edge with an automated program, in order to correctly include more counts, does not lower the SEE as hoped. This result is in contrast to the results of others with different data and a manual method. Possible causes for the difference are given.

Key words: left-ventricular volume, attenuation correction, linear attenuation coefficient, region of interest, ^{99m}Tc

INTRODUCTION

A previous paper by Rabinovitch *et al.*[1] presented a critical appraisal of calculation of left-ventricular volume by the count-based method utilizing *in vivo* red-blood-cell labeling with ^{99m}Tc.[2] They compared scintigraphic volume measurements from 26 adult patients to measurements from biplane contrast ventriculography. The patients were imaged with a parallel-hole collimator in both the left anterior oblique (LAO) and the left posterior oblique (LPO) positions. The former images were used to compute the counts for the left ventricle and the latter images to allow patient-by-patient attenuation correction. In the present paper, we investigate the data further with respect to variations in the calculation of ventricular volume.

Rabinovitch *et al.*[1] report that attenuation correction with a linear attenuation coefficient of 0.15 cm^{-1}, the value for water, improves the correlation of contrast volume with radionuclide volume. However, Links *et al.*[3] have found that, even with attenuation correction, using $\mu = 0.15$ cm^{-1}, and employing the same automated second-derivative edge-detection program used by Rabinovitch *et al.*, one obtains volumes which are consistently smaller than the "true" volumes, as given by angiographic measurement. They presented a manual approach which purposely extended the region-of-interest (ROI), especially along the lateral and inferior margins of the left ventricle, in order to include as many of the counts under the tails of the point spread function as possible without including counts from other chambers of the heart. They did obtain better results for ten patients but also felt that high intraobserver variability with their manual method could be a limitation.

Rabinovitch *et al.*[1] also make mention of the fact that optimizing the value of a single linear attenuation coefficient further improves the correlation value, and they briefly discuss the optimum values and their significance.

In this paper, we (1) examine two methods of calculating depth from the skin surface to the center of the left ventricle (LV), (2) investigate both the use of a single attenuation coefficient and the use of two uniform attenuation coefficients, one for the blood pool and a smaller one for the region between the heart and the camera, (3) optimize the value(s) of the attenuation coefficient(s), and (4) increase the counts recorded for the ventricle by expanding the LV region of interest in a manner which seeks to mimic the end result of Links *et al.* For the expansion, we have developed a new automated program which starts from the region found by second-derivative techniques. An automated program could potentially produce a method with low intraobserver variability. Two statistics are used for evaluating the quality of results.

METHOD

Study population

The study group consists of 26 adult patients: 23 males and 3 females, with a mean age of 53 years. Twenty-one patients have coronary artery disease, three have aortic insufficiency, and one has congestive cardiomyopathy.

Angiography

All patients undergo biplane contrast cineventriculography in the 30° right anterior oblique (RAO) and 60° LAO

 0094-2405/85/010093-06$01.20

projections. Just prior to cineangiography, the distances from the mid-left ventricle to the RAO and LAO image intensifiers are determined using the left-ventricular catheter as a guide. Corresponding RAO and LAO image magnification factors are determined from previously constructed curves utilizing a 1-cm-square calibration grid. Left-ventricular end-diastolic (ED) and end-systolic (ES) edges are manually traced from the appropriate frames. All premature and immediately postpremature beats are excluded from the analysis. Contrast left-ventricular ED and ES volumes are then calculated by the area–length method.[4,5]

Radionuclide imaging technique

Radionuclide imaging takes place within one day of cardiac catheterization in 22 patients, within two days in three patients, and within seven days in one patient. The patients' clinical status and medications are the same during both studies.

Gated equilibrium cardiac blood pool scintigraphy is performed after *in vivo* red-blood-cell labeling with 25 mCi (925 MBq) of Tc-99*m*.[2] All images are obtained with a standard field-of-view Anger camera interfaced with a minicomputer. To minimize camera–computer deadtime losses, an annular lead shield (internal diameter 16.5 cm and external diameter 30.5 cm, thickness 3 mm) is placed on the collimator face. With the patient in the supine position with his left side against a 45 ° wedge, a 28-frame LAO study is acquired in 32×32 matrix, and then interpolated to 64×64 with a commercial software program. The study is acquired with a low-energy medium sensitivity parallel-hole collimator and contains 150–200 K counts/frame. Following this, while the patient is still in the LAO projection, a Co^{57} marker source is positioned on the chest wall to coincide with the center of the left-ventricular blood pool on the persistence scope. A short static image is obtained to verify position. Next, without moving the patient, the orthogonal 28-frame gated LPO study is obtained using the parallel-hole collimator with 100–150 K counts/image. A 5-ml sample of peripheral venous blood is obtained from the arm opposite the injection sites immediately after LAO acquisition (before placement of the marker). After completion of the LPO study, the blood sample is counted on the face of the parallel-hole collimator for 60 s and results corrected for decay corresponding to the time between the LAO acquisition and the blood sample counting.

Second-derivative region of interest and background estimation

The LAO images are analyzed employing the high-resolution option of a commercial second-derivative algorithm (Medical Data System MUGE). This algorithm determined ventricular edges either through the zero crossing of the directional second derivative of the image intensity averaged over all directions or, if this is unsuccessful, at an operator-set threshold value. A preliminary background region of interest is generated lateral and inferior to the left ventricle. From this analysis, the frame with peak counts is chosen as the ED image and the frame with minimum counts is chosen as the ES image. The ROIs for these images are saved.

In order to finally correct for background activity, we employ one of three methods. The first, introduced by Rabinovitch *et al.*, estimates background from the ES image in the following way. The most superior and inferior points within the region of interest generated by the second-derivative algorithm are noted. Three profiles are drawn through the image at equally spaced intervals between these points. Then for each profile, the five pixels to the right of the region of interest are examined for their minimum value. The minimum values for the three profiles are then averaged to produce an estimate of average background counts/pixel. This background density, determined from the ES image, is applied to both the ES and the ED frame. The middle profile and minimum value for a typical ES study are shown in Fig. 1.

Secondly, we examine the effects of using only two profiles, the most superior and the middle one, to compute the average background, and thirdly we employ a background region lateral and inferior to the expanded region of interest.

Attenuation correction

Three methods for calculating attenuation correction from the LPO images are tested. In each method, all counts measured are assumed to be located at a single point within the ventricle. That is, we do not attempt to correct for the varying attenuation of activity due to different locations within the ventricle.

In the first method, a composite functional image, consisting of the sum of the difference image (ED − ES, with nega-

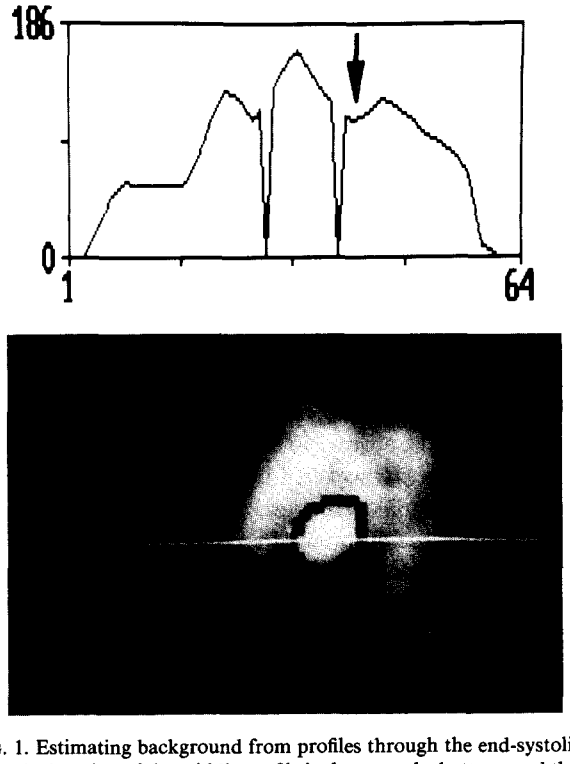

FIG. 1. Estimating background from profiles through the end-systolic image. The location of the middle profile is shown at the bottom, and the plot of counts vs pixel number is shown at the top. A sharp drop to zero counts marks a second-derivative edge. The black arrow indicates the minimum count in the profile within five pixels of the edge; this count value is part of the background estimate.

tives set to zero) and the paradox image[6] (ES − ED, with negatives set to zero), is used to delineate the mitral valve plane. The midpoint between this plane and the apex of the ventricle is determined and then the distance d (in cm) from this midpoint to the chest marker is found. Attenuation correction is made by multiplying by the factor

$$F = e^{\mu d},$$

where μ is assumed attenuation coefficient.

In order to obtain a more representative average depth, for the second procedure,[3] an ellipse is located around the ventricle and a count-weighted depth determined from the points within the ellipse by the formula

$$d = \frac{\Sigma C_i d_i}{\Sigma C_i}.$$

Here, C_i are the counts located at depth d_i. Attenuation correction is then made by multiplication by the same factor as in the first method.

In the third method, the count-weighted depth is calculated but, in addition, the depth from the displayed central point to an inferior–superior line through the apex d_I is also measured. Then the depth from this line to the chest marker d_E is given by $d_E = d - d_I$. Finally, the factor used for correction is given by

$$F = e^{\mu_E d_E} e^{\mu_I d_I},$$

where μ_E is the assumed external attenuation coefficient and μ_I is the assumed internal (blood pool) attenuation coefficient.

Automated program for expanding the ROI

The new automated program for expanding the LV region of interest has three main features. (1) It starts from the second-derivative ROI. (2) It expands the region stepwise according to a fixed algorithm, keeping track of the intermediate results until a fixed number of steps has been completed. It uses a similar algorithm to find a background estimate region. (3) Using a background count estimate computed from the background estimate region or a background from another image, it then checks the stepwise expansion against a stopping criterion. From the stopping criterion, it determines whether the region should be taken as that from the full expansion or that at one of the intermediate steps. Details are found in the Appendix.

A typical result for an ED image is presented in Fig. 2. The original image is shown at the left. The result of the full expansion is shown in uniform grey in the image at the right with the starting, second-derivative edge superimposed as black. The bright region at the lower right is the background region. For this case, the stopping criterion was not met and the expanded region goes right up to the background region.

Tests run

A large number of combinations of the methods described in the previous sections exist for calculation of the ventricular volume. We report on many of them but do not attempt to exhaustively cover all possibilities. In most tests, we use background determined from the ES image for the ED calculation; the rationale for this usage is that examining pixels just outside the region of the ES ventricle should give a good estimate of background under the ED ventricle. Rabinovitch *et al.* used the depth derived from the functional image and assumed an *a priori* value for μ of 0.151 cm^{-1}. We report this case in our results for comparison. They also made a preliminary report on one of the methods used in this paper, varying μ to improve the correlation with the contrast volumes. This report expands on that result and includes the use of a μ_E–μ_I pair. The procedure followed for both optimizations is to step through the values of the attenuation coefficient(s) in steps of 0.01 cm^{-1} and calculate resultant radionuclide volumes. Then, one should correlate contrast volumes against these resultant volumes and make note of the values of the standard error of the estimate (SEE) as given by

$$\text{SEE} = \left[\frac{1}{N}\sum_{i=1}^{N}(A_i - E_i)^2\right]^{1/2},$$

where A_i is the contrast volume for the ith patient, E_i is the value of the contrast volume from the best-fit equation evaluated at R_i, the radionuclide volume for the ith patient, and N is the number of patients. The adjustment of attenuation coefficient is continued until a minimum in SEE is found or the coefficient reaches zero. (In the case of the μ_E and μ_I

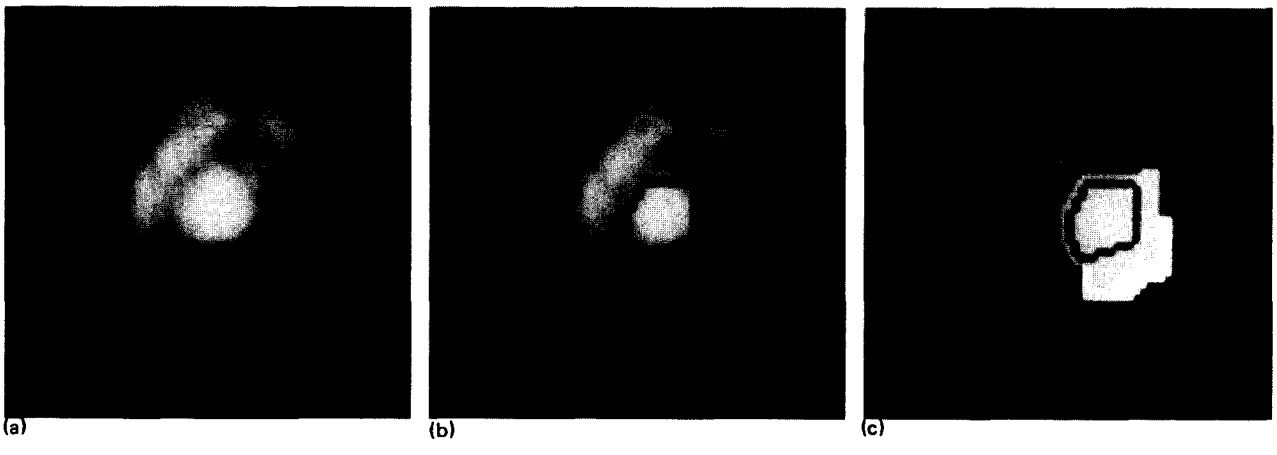

FIG. 2. Typical result for the automatic region expansion program. (a) The original end-diastolic image. (b) The image with the second-derivative region shown enclosed by a black line. (c) The image, starting region, and a uniform grey region which marks the result of the expansion. The bright white region in the lower right is defined automatically by the algorithm and is the part of the image used for background estimation.

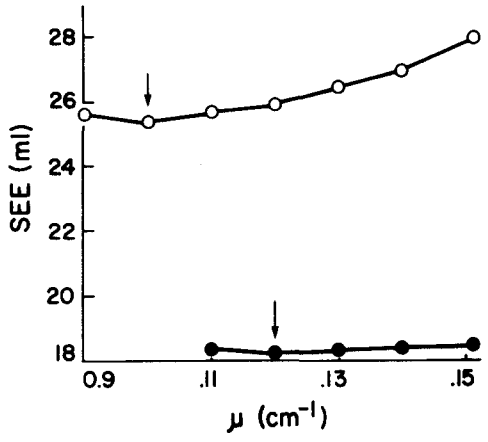

FIG. 3. The dependence of the standard error of the estimate (SEE), from the correlation of contrast volumes with radionuclide volumes is shown as a function of assumed attenuation coefficient μ for ED (○) and ES (●) data (test 2 of Tables I and II, respectively). The arrows mark the minima.

pair, both are varied toward zero with the additional requirement that $\mu_E \leqslant \mu_I$.)

We also examine the root-mean-square difference (RMSD) between the angiographic and radionuclide results. This statistic is computed as

$$\mathrm{RMSD} = \left[\frac{1}{N}\sum_{i=1}^{N}(A_i - R_i)^2\right]^{1/2},$$

and measures how well the radionuclide and contrast methods give identical volumes (i.e., to what extent the best-fit line goes through the origin and has a slope of 1).Note that the RMSD was evaluated at the minimum SEE. If the optimizations were carried out to minimize RMSD, lower values might result without too much degradation in the SEE.

RESULTS

For ED, the range of contrast volumes is 92–646 ml with a mean of 172 ml and a standard deviation of 111 ml. For ES, the range is 27–548 ml with a mean of 77 ± 104 ml.

An example of the radionuclide ED and ES results from minimizing SEE as a function of μ in the case of the second-derivative ROI, the functional image depth, and the three-profile background is shown in Fig. 3. The slow variation is typical of the optimization for all cases tested.

The results from assuming a fixed value of μ and from minimizing SEE as a function of μ for the ED and for the ES images are given in Tables I and II, respectively. The tables reveal that no tested variation upon the simplest assumption of an *a priori* μ equal to 0.151 cm^{-1} gives results with both a smaller SEE and a smaller RMSD. In the tests with the second-derivative region of interest, the SEE is reduced slightly at the optimum μ (test 2–4 for Table I and test 2 for Table II) or optimum pair of μ's (test 5, Table I) compared to μ equal to 0.151 cm^{-1} (test 1 for both tables). For the ED phase (Table I), the SEE resulting from optimizing both μ_I and μ_E (test 5) is not better than the SEE obtained by optimizing a single μ (test 2). The best ED-phase SEE is thus 25 ml at a μ of 0.10 cm^{-1}, and the best ES-phase SEE is 18 ml at a μ of 0.12 cm^{-1}. A scatter plot of contrast volume versus radionuclide volume is shown in Fig. 4 for the ED case.

In the tests with the expanded region of interest, the SEE is always worse than an existing comparable case with the second-derivative region of interest. Moreover, only in the case of the ED phase and a pair of μ's does the expanded region (test 8, Table I) reduce the RMSD at the minimum SEE, compared to that when using the second-derivative region (test 5, Table I).

When using a single optimized attenuation coefficient in the ED phase, the following additional comments can be made: with a three-profile background, for ED images, the weighted method of depth calculation produces a slightly worse SEE (28 ml) than that (25 ml) from the functional image method. When using a functional image depth, the two-profile background produces a slightly worse SEE (27 ml) than the three-profile background (25 ml).

DISCUSSION

The best SEEs for both the ED and ES heart phase are obtained with a single optimized μ and the standard second-

TABLE I. Results from tests of calculation variation for ED images.

Test	Region	Background Image	Background Method	Depth	Attenuation coefficients (cm^{-1}) μ	μ_I	μ_E	SEE (ml)	RMSD (ml)
1	Second derivative	ES	3 profiles	Functional image	0.151[a]			29	42
2	Second derivative	ES	3 profiles	Functional image	0.10			25	94
3	Second derivative	ES	2 profiles	Functional image	0.11			27	73
4	Second derivative	ES	3 profiles	Weighted	0.11			28	86
5	Second derivative	ES	3 profiles	Weighted		0.151	0.07	27	84
6	Expanded	ES	Region	Functional image	0.07			42	106
7	Expanded	ED	Region	Functional image	0.11			39	61
8	Expanded	ES	Region	Functional image		0.151	0.07	41	66

[a] Was not varied but fixed at this value.

TABLE II. Results from tests of calculational variations for ES images.

Test	Region	Background Image	Background Method	Depth	Attenuation coefficient μ (cm^{-1})	SEE (ml)	RMSD (ml)
1	Second derivative	ES	3 profiles	Functional image	0.151[a]	22	20
2	Second derivative	ES	3 profiles	Functional image	0.12	18	38
3	Expanded	ES	Region	Functional image	0.04	29	76

[a] Was not varied but fixed at this value.

derivative edge. If one is evaluating only the ED phase, then the optimum value for μ is 0.10 cm^{-1}, while if one is evaluating only the ES phase, then the best value for μ is 0.12 cm^{-1}. The larger attenuation coefficient for the ES phase, where the centroid of the ventricle is presumably deeper in from the skin surface, is at first somewhat surprising. A larger attenuation is expected for this phase but one could assume that this would be entirely taken care of by a greater measured depth. Our larger μ may partly be compensating for underestimation of the depth, or it may be reflecting some different scatter condition.

The best single value for correcting all phases is a simple average of the above two values, or 0.11 cm^{-1}. This average value agrees with the mean minus one standard deviation value found in the independent study of Nickoloff *et al.*[7] Their value of 0.13 $cm^{-1} \pm 0.02$ (1 SD) cm^{-1} was obtained by evaluating the CT scans of the thorax for 11 patients and mathematically converting from x-ray energies to the linear attenuation coefficient at 140 keV. In a related comparison, the average value reported here is 0.02 cm^{-1} larger than the empirical value of 0.09 cm^{-1} found to be optimum for attenuation correction in single-photon-emission tomography of sources in the dog's thorax.[8] Both bronchial tree point sources and a long esophageal line source were investigated for absolute quantification.

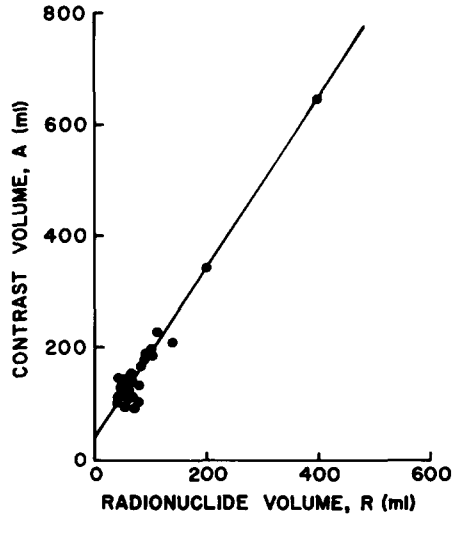

FIG. 4. A scatter plot of contrast volume vs radionuclide volume for ED using a second-derivative region, a three-profile background from the ES images, a depth from the functional image, and a single optimized attenuation coefficient of 0.10 cm^{-1}. The equation of the best-fit line is $A = 39.33 \pm 1.51\ R$. The correlation coefficient is 0.97 and the standard error of the estimate is 25 ml.

These studies, then, all argue in favor of the use of values less than 0.15 cm^{-1}. However, in this work, the RMSDs at the optimum SEE were worse than with the *a priori* μ, so that using the optimum attenuation coefficients may not be desirable when it is important that the absolute values of the volumes be correct. If these absolute values of volume are of primary concern, then an optimization of μ for the smallest RMSD would be called for.

The optimum values of the $\mu_I = 0.15$ cm^{-1} and $\mu_E = 0.07$ cm^{-1} for the ED heart phase reported here agree less well with the CT results of Nickoloff *et al.*, which give $\mu_I = 0.15$ cm^{-1} but $\mu_E = 0.12$ cm^{-1}.[9] This less good agreement, and the fact that employing an external and an internal linear attenuation coefficient did not improve SEE results further are probably due to the extra errors introduced by measuring two depths.

Links *et al.* found that manually expanding their left-ventricular regions of interest appeared to give better values for their computed end-diastolic volumes. Using their data (a randomly selected subset consisting of ten patients), as found in Table 3 of Ref. 3, our analysis gives similar results. Correlating contrast volume with radionuclide volume, the SEE is 32 ml for the second-derivative regions, and drops to 20 ml for the manual, expanded regions. Moreover, the RMSD is 72 ml for second-derivative regions and drops to 30 ml for the manual, expanded regions. It would appear that a better correlation occurs as more counts are correctly included in the regions.

We tried to attain a similar improvement with a semiautomated program, in order to help ensure low intraobserver variability. With this program and with our data, the SEE is worse compared to comparable methods using standard second-derivative regions. Possible reasons for the differing results are as follows. (1) The use of the second-derivative program by Links *et al.* was significantly different from ours. We used a profile background, while they used the region background defined by the second-derivative program. Moreover, their original regions might have been too small, giving room for improvement by expanding the region. (2) The new automated program did not produce results which mimic the results of the manual method. (3) The two data sets had characteristics which differed in a critical way. The

data presented here did employ the lead annulus for reducing deadtime and thus did not permit choosing a background region at a great distance from the ventricle.

We conclude that, if one assumes that the angiographic volumes are correct, it is quite difficult to discover consistent calculational variations which lead to improvements in radionuclide results. The multiple variables of region, background, depth, and attenuation correction combine to make such discovery difficult. Whether reducing Compton scattering by the use of an asymmetrically high window would help the situation has not been addressed in the present investigation.

ACKNOWLEDGMENTS

The authors would like to acknowledge that the original idea for using the comparison of uptake increment to likely error as a stopping criterion was due to Dr. W. Leslie Rogers. We are also grateful to Ms. Diane Vecellio for her excellent secretarial assistance.

APPENDIX

In detail, the procedure for the automated ROI expansion is as follows. The simple (not count-weighted) centroid of the second-derivative region of interest is found and the image is divided into sections by radial lines emanating from the centroid point. If the superior direction in the image is called 0° and angles are measured from this direction with clockwise positive, then from 50° to 180° defines the major expansion sector, the remainder of the total angle defines the minor expansion sector, and from 100° to 180° defines the background expansion sector. Major and minor growth of the left-ventricular ROI is based upon an expansion into all pixels which are both nearest neighbors of an already included pixel, and also within the major or minor expansion sector, respectively. The nearest neighbors are the eight pixels closest to a pixel. (The use of nearest neighbors and the technique for carrying out the processing is the same as that used for adrenals in Ref. 10).

The program starts with a single expansion into the minor expansion sector, followed by three successive expansions into the major expansion sector. To define the background region, two further expansions are made into all pixels which are both nearest neighbors of either a ventricular pixel or a newly found background pixel, and also within the background expansion sector. Provision is also made for accepting a background count estimate as previously determined from analyzing an image from a different phase of the heart cycle.

The background region is prevented from including pixels whose count value has been reduced by the deadtime shield. This possibility was only a problem in the one case where the ED image was used for background; a manual, operator-interactive assessment of the edge of the image was made for this one test.

Values for the stopping criterion are computed as follows: The Poisson statistics errors in the total counts and in the background estimate are calculated. From these, using propagation of error, the error in the background-subtracted number of counts (or net counts) is computed. The stopping criterion is to stop if the number of counts added to the net counts in the present iteration is less than the net-count error in the previous iteration.

[a] Address reprint requests to Kenneth F. Koral, Ph.D., Division of Nuclear Medicine, University of Michigan Medical Center, 1405 E. Ann Street, Box 021, Ann Arbor, MI 48109.

[1] M. A. Rabinovitch, V. Kalff, K. F. Koral, W. Chan, J. E. Juni, B. Lerman, R. Lampman, J. Walton, D. Grassley, R. Vogel, B. Pitt, and J. H. Thrall, Radiology **150**, 813 (1984).
[2] D. G. Pavel, A. M. Zimmer, and V. N. Patterson, J. Nucl. Med. **18**, 305 (1977).
[3] J. M. Links, L. C. Becker, J. G. Shindledecker, P. Guzman, R. D. Burrow, E. L. Nickoloff, P. O. Alderson, and H. N. Wagner, Circulation **65**, 82 (1982).
[4] H. T. Dodge, H. Sandler, D. W. Ballew, J. D. Lord, Jr., Am. Heart J. **60**, 762 (1960).
[5] W. J. Rogers, L. R. Smith, W. P. Hood, Jr., J. A. Mantle, R. O. Russell, Jr., and C. E. Rackley, Circulation **59**, 96 (1979).
[6] B. L. Holman, J. Wynne, J. Idoin, J. Zielonka, and J. Neill, J. Nucl. Med. **20**, 1237 (1979).
[7] E. L. Nickoloff, P. D. Esser, W. H. Perman, B. Bashist, and P. O. Alderson, Med. Phys. **10**, 523 (1983)(Abstract).
[8] D. Osborne, R. Jaszczak, R. E. Coleman, K. Greer, and M. Lischko, J. Nucl. Med. **23**, 446 (1982).
[9] E. L. Nickoloff (private communication).
[10] K. F. Koral, H. Abukhadra, M. Tuscan, and W. H. Beierwaltes, Comput. Programs Biomed. **15**, 73 (1982).